A physically based strength prediction model for glass

Jonas Rudshaug[1,2], Odd Sture Hopperstad[2], Tore Børvik[1,2]

[1]Norwegian Defense Estates Agency, National Center for Protection of Buildings, Norway
[2]Structural Impact Laboratory (SIMLab), Department of Structural Engineering, NTNU Norwegian University of Science and Technology, Norway

The strength of glass has been a subject of great interest for more than one hundred years. Due to the stochastic nature of glass, originating from microscopical surface flaws, glass plates exhibit large variations in fracture strength. The aim of this work is to present a new strength prediction model for glass, named the Glass Strength Prediction Model (GSPM) that captures the nature of fracture initiation in glass, spanning from rate dependence to size effects. We aim for the presented model to be applicable in modern design processes and provide a procedure to facilitate input parameter calibration for glass plates from different suppliers. GSPM is a Monte-Carlo based model that combines the theories of linear elastic fracture mechanics (LEFM) and sub-critical crack growth (SCG) to generate virtual tests on a representative sample of glass plates. The stress evolution in the glass plates is obtained from finite element (FE) simulations. The model results in representative fracture strength distributions that span the probable fracture initiation instances with respect to time, location and stress level. We demonstrate how the GSPM can be used to trigger fracture in the constitutive model MAT_280 in LS-DYNA. This feature provides the option to investigate scenarios including multiple glass plates with interdependent fracture initiation behavior. The GSPM displays great promise in terms of usability and prediction capacity. It can capture the fracture initiation behavior of glass plates of varying geometries exposed to load cases spanning from, e.g., quasi-static four-point bending to blast pressure. The model has the potential to reduce the number of physical experiments and numerical FE simulations in modern development processes of glass structures.

1 Introduction

Modern cars tend to include an increasing number of windows, with the aim to provide the passengers views in all horizontal directions as well as a sky view. The windows are made of curved glass plates, either monolithic or laminated. In extreme load cases, like real car-crashes or the NCAP-evaluation tests (NCAP, 2023), the windows influence the structural capacity of the car. To predict the performance of a car in an extreme load case scenario, we need to estimate the strength of the windows, i.e., when the windows fracture. It is well known that the strength of glass plates is stochastic, a feature that stems from microscopical cracks distributed on the plate surfaces [1-5]. The consequence of the stochastic strength of glass plates is that every instance exhibits a unique fracture behavior. Several models have been proposed with the aim of predicting the fracture strength of glass [2, 6-18]. Most of the models are based on a combination of sub-critical crack growth (SCG) and fracture strength based on the Weibull probability distribution function (PDF) [1]. However, the Weibull PDF does not always properly represent the fracture strength distribution seen experimentally. Yankelevsky [2] proposed an approach based on the fact that the probabilistic fracture behavior of glass originates from varying surface flaw distributions, or flaw maps, of glass plates. To imitate this behavior, the model produces a set of virtual flaw maps with varying flaw shape, size and location. The fracture strength is found by combining the information from the flaw maps and linear elastic fracture mechanics (LEFM) theory. Later, other models predicting failure in glass based on flaw maps have been proposed [20-23]. The models predicting fracture initiation in glass based on flaw maps do not take SCG into account. In addition, they are not validated for complex plate geometries. Kinsella and Serrano [3] proposed a flaw map-based model coupled with SCG, combining features from both families, and validated the model to ring-on-ring and ball-on-ring experiments.

The models mentioned above focus on finding the probability of failure, in terms of fracture initiation, and are only validated for flat glass plates. In addition, they do not consider the post-failure stage. In extreme load cases, like real car crashes or the NCAP-evaluation tests [4], the plate geometries are complex, and both the pre- and the post-failure stages need to be considered. Brokmann [5] developed a model based on SCG and initial flaw sizes estimated from fracture stresses fitted to a Weibull PDF. The model was used to predict the failure strength of windshields and implemented as a user material model into an FE code, making the model more user friendly. Rudshaug et al. [6] proposed a new Glass Strength Prediction Model (GSPM) that builds on the foundation laid by Yankelevsky [2] and Osnes et al. [7, 8]. GSPM is a model with improved predicting capacity that combines the use of virtual flaw maps to describe the probabilistic fracture behavior of glass and SCG.

In this paper, we present a brief presentation of the GSPM and details of the implementation of the model into MAT_280 in LS-DYNA R12. The reader is referred to [6] for a more detailed presentation.

2 Glass strength prediction model

The GSPM predicts fracture initiation in an FE simulation using LEFM and SCG in a Monte Carlo framework. The key feature of the GSPM is a generated representative sample of artificial flaw maps on the glass plate surfaces, which lays the foundation for the fracture strength predictions. The generated flaw maps each contain flaws based on the selected flaw density, with a defined shape, depth, orientation and location. Based on the loading history, the model keeps track of the predicted sub-critical growth of each flaw originating from mode I-loading and predicts when and where failure occurs for each flaw map in the generated representative sample. The model implementation is based on an explicit FE framework, where glass plates are modeled using shell elements.

The model is implemented into LS-DYNA as an extension to MAT_280. The extension allows the user to take the stochastic nature of glass into account during FE simulations without the need to run multiple simulations. At the start of the FE simulation, the GSPM generates a representative sample of the simulated glass plates covered with artificial flaw maps. Using this representative sample in combination with the progressing loading history, the GSPM outputs a failure distribution which is naturally sorted from weakest to strongest. With this property, the user can select a relative strength of the glass specimen. Until the virtual specimen representing the selected strength fails, the model predicts a scatter in the fracture initiation location and time for the weaker virtual specimens, which provides an idea of the repeatability of the studied case. A small scatter implies a repeatable strength for the given load case and geometry in question. The predictions can be used to trigger fracture in constitutive models at a physically based time and location. This flexible way of including the stochastic nature of fracture initiation of glass plates in numerical simulations makes it applicable in numerous design applications.

2.1 Flaw generation and distribution

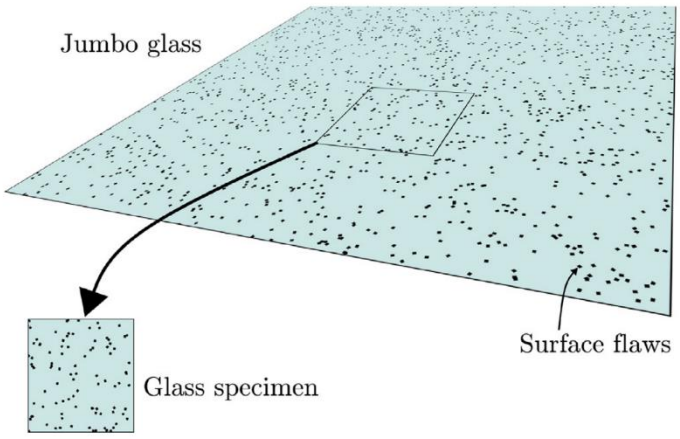

Fig.1: Illustration of the flaw generation and distribution procedure in the GSPM. Adopted from [6]

To represent the flaw distribution found on the surfaces of a glass plate specimen, we have based the flaw generation procedure on the float glass production line. In a typical float glass production line, glass melt is poured onto a large tin bath, forming a so-called jumbo glass plate, with typical dimensions of 3.12 m × 6 m [9]. During the solidification of the glass melt, small microscopical flaws, invisible to the naked eye, are created on the glass surface. A consequence of the production process is that the two glass plate surfaces are not identical. The tin side has been found to be marginally weaker that the air side [9, 10]. However, as a simplification, both glass surfaces are assumed to have equal flaw distributions. After solidification and cooling, the jumbo glass plate is cut into smaller glass specimens. In the GSPM, this process is emulated by first creating a jumbo glass plate of a user specified area, A_{jumbo}. Second, we generate N_0 flaws on each of the jumbo glass plate surfaces based on shape, size,

and orientation distributions. Third, we cut the jumbo glass plate into smaller glass specimens of areas $A_{specimen}$, as illustrated in *Fig. 1*. The parameters governing the flaw distribution are presented in *Table 1*Table 1: (parameters 1–3). The number of virtual jumbo glass plate flaw maps, M_{jumbo}, is given by

$$M_{jumbo} = \left\lceil M_{it} \frac{A_{specimen}}{A_{jumbo}} \right\rceil \quad (1)$$

where $\lceil x \rceil$ is the ceiling function and M_{it} is the number of glass specimen flaw map iterations. The number of flaws per jumbo glass plate, N_0, is given by

$$N_0 = \rho_{\mathrm{flaw}} \mathrm{A}_{\mathrm{jumbo}} \quad (2)$$

where ρ_{flaw} is the surface flaw density.

We assume that the flaws are non-interacting and uniformly distributed over the glass surface. In addition, we assume that the distance between the flaws is much larger than the dimensions of single flaws. To fulfill the assumptions that the flaws are uniformly distributed on the glass surfaces, we draw the location of each flaw based on a unique random selection of the elements hosting flaws of the glass plate mesh from the FE simulation. In other words, for each virtual flaw map on the glass plate surfaces, we perform a random selection of elements that contain a flaw. The random selection is done using Floyd's algorithm for sampling without replacement [11]. By assuming that the element size is uniform, the drawn positions are distributed uniformly on the glass surface. We assume that there is a single flaw of the largest depth in the jumbo glass plate, and an increasing number of flaws for decreasing flaw depths. The depth distribution is given by

$$\frac{N_i}{N_0} = exp\left(-\frac{a_i - a_{min}}{\eta}\right) \quad (3)$$

where a_i is the depth of flaw i, a_{min} is the minimum flaw depth of the flaw distribution, N_0 is the total number of flaws on the jumbo glass plate surface, N_i is the number of flaws that have depths larger or equal to a_i, and η is a distribution parameter given by

$$\eta = \frac{a_{max} - a_{min}}{ln(N_0)} \quad (4)$$

where a_{max} is the maximum flaw depth of the flaw distribution.

2.2 Procedure

The strength prediction procedure of the GSPM is presented schematically in *Fig. 2* and *Fig. 3*. Below follows a stepwise walk-through of the procedure:

1. At the start of the simulation, we generate and distribute flaw maps for M_{it} unique artificial glass plate specimens, see *Fig. 2*. These flaw maps serve as a representative sample for glass plate specimens of the same kind.
2. We enter a prediction loop, see *Fig. 3*, where the presented procedure is repeated for each stress frame until the failure criterion is met:
   (a) Calculate the current time step based on the simulation time step and potential time scaling, retrieve the current stress field and initiate the flaw map counter, $m = 1$.
   (b) Apply surface flaw map m to the current stress field.
   (c) Loop through every flaw in the intact artificial glass samples, calculate the stress intensity for mode I-loading, K_i, and perform one of the following actions:
   - $K_I < K_{th}$
     The flaw remains unchanged.
   - $K_{th} < K_I < K_{IC}$
     The flaw grows sub-critically. We update the flaw depth and length based on SCG theory with a depth evolution given by
     $$v = \frac{\mathrm{d}a}{\mathrm{d}t} = v_0 \left(\frac{K_I}{K_{IC}}\right)^n \quad (5)$$
   - $K_I > K_{IC}$
     The flaw grows over-critically and at this point we predict that failure has occurred for the artificial glass sample. We save the failure information and remove the glass sample from the collection of intact samples. If multiple flaws are critical at the same time step, the flaw failing first is considered the most critical, which is decided based on the linearly approximated time at

failure, t_f, given by

$$t_f = t_{i-1} + \frac{K_{IC} - K_{I,i-1}}{K_{I,i} - K_{I,i-1}}(t_i - t_{i-1}) \quad (6)$$

where the indices $i-1$ and i represent the previous and current time step.

If $m < M_{it}$, increment the flaw map counter and go to (b) else, finish time step.

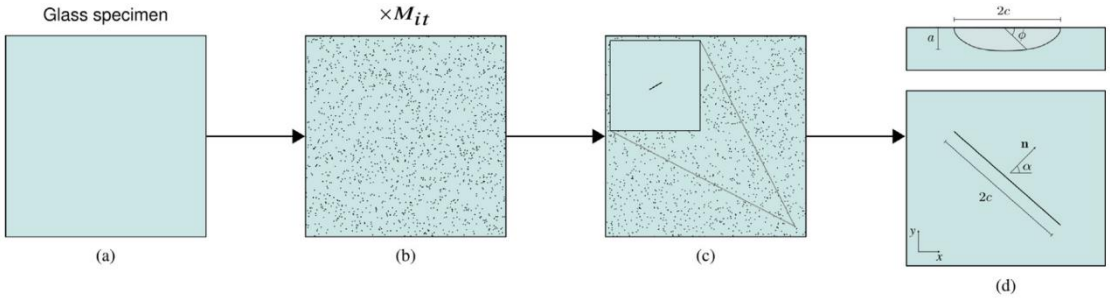

Fig.2: Illustration of flaw map generation: start with the glass specimen geometry (a) and generate M_{it} flaw maps (b) where each flaw has a depth, a, length, $2c$ and orientation, α, (c-d). Adopted from [6].

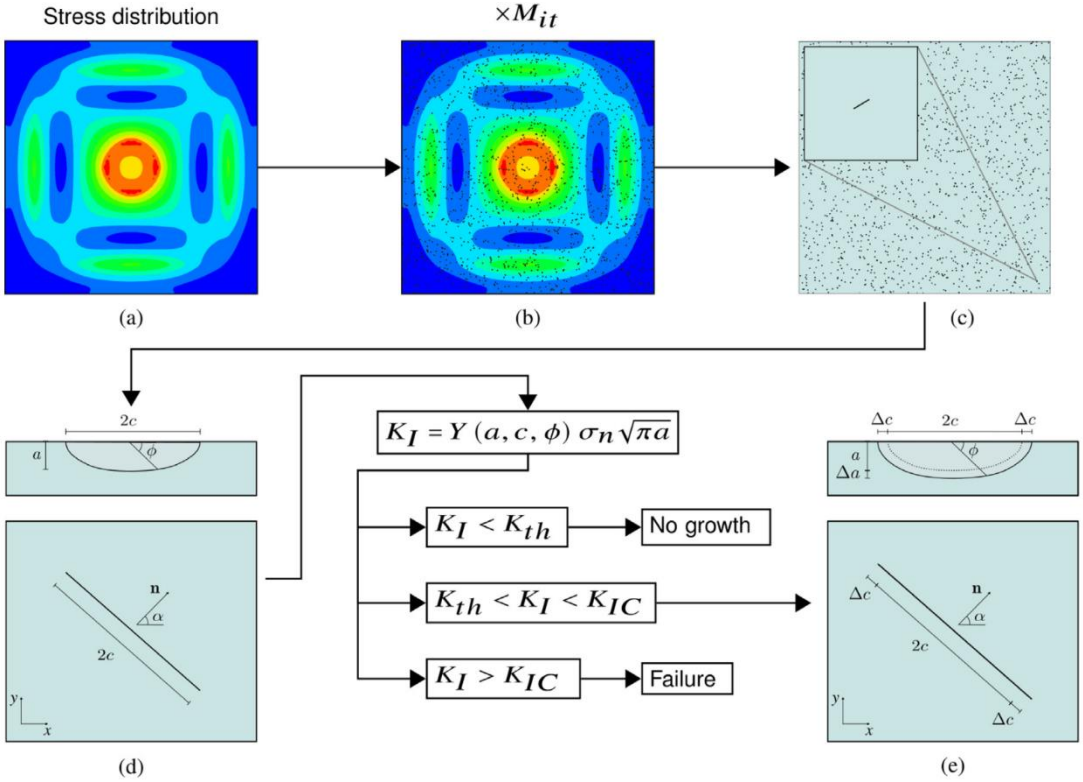

Fig.3: Schematic illustration of the prediction loop for a stress frame: starting with the stress distribution (a), each of the M_{it} virtual flaw maps are mapped onto the stress distribution (b), where each flaw is investigated for potential SCG or failure (c–e). Adopted from [6].

3 Implementation in LS-DYNA

The addition of the GSPM as an extension of MAT_280 in LS-DYNA introduces the possibility of a stochastic handling of fracture initiation in the material model. Contrary to the present stochastic extension available in MAT_280 with one instance of spatially varying tensile strength, the GSPM makes use of a representative sample of glass plates in its predictions. Every instance in the representative sample of glass plates produced by the GSPM is exposed to the same load history, each initiating fracture at a specific time, location and fracture stress influenced by its unique flaw map. The resulting naturally sorted fracture strength distribution that evolves during a simulation is used to select a glass plate strength based on the model input. In the extension, the GSPM predicts the tensile strength, the initiation location and the initiation time for the first crack and communicates the information to MAT_280. Then MAT_280 takes over and predicts the resulting crack propagation from the point predicted by GSPM. *Table 1* presents the input parameters of the GSPM related to flaw distribution (1-3), flaw shape (4-9), SCG (10-13), time scaling, noise handling and update frequency (14-16) and the fracture strength (17).

Table 1: The GSPM input parameters related to the flaw distribution (1–3), flaw shape (4–9) and SCG (10–13). Time scaling, noise handling and update frequency parameters (14–16) and the fracture strength parameter (17) are also presented. Adapted from [6].

Number	Variable	Symbol	Description	Unit
1	NUMIT	M_{it}	Number of glass specimen flaw map iterations	[-]
2	JUMAR	A_{jumbo}	Area of a jumbo glass plate	[mm^2]
3	FDENS	ρ_{flaw}	Flaw density	[flaw/mm^2]
4	FDMIN	a_{min}	Minimum flaw depth	[mm]
5	FDMAX	a_{max}	Maximum flaw depth	[mm]
6	ACMN	$(a/c)_{mean}$	Flaw depth-to-half-length ratio, mean value	[-]
7	ACSTD	$(a/c)_{std}$	Flaw depth-to half-length ratio, standard deviation	[-]
8	ACMIN	$(a/c)_{min}$	Flaw depth-to-half-length ratio, minimum value	[-]
9	ACMAX	$(a/c)_{max}$	Flaw depth-to-half-length ratio, maximum value	[-]
10	KCRIT	K_{IC}	Critical stress intensity	[MPa $\sqrt{\text{mm}}$]
11	KTH	K_{th}	Stress intensity threshold for SCG	[MPa $\sqrt{\text{mm}}$]
12	V0	v_0	Terminal SCG speed	[mm/s]
13	N	n	SCG exponent	[-]
14	TSCL	t_{scale}	Time scaling factor	[-]
15	EXPA	α_{exp}	Exponent for moving exponential averaging	[-]
16	NINC	n_{inc}	Number of increments to skip per GSPM update	[-]
17	FPERC	P_f	Failure percentile	[-]

3.1 Quasi-statically loaded windshield

A possible use case for the GSPM expansion of MAT_280 is to predict the outer limits of the strength of a quasi-statically loaded windshield. In this example, the windshield is subjected to a wooden impactor with a diameter of 200 mm at a speed of 13 mm/min in the center of the windshield. A test series of eleven windshield tests [12] was used to calibrate the input parameters. We ran two simulations to investigate the outer limits of the windshield strength for the given load case. One with a failure percentile

value P_f = 0.05 for both glass layers, and one with P_f = 0.95. The f_t parameter in MAT_280, determining the tensile strength after the first crack, was set to 30 MPa for P_f = 0.05 and 75 MPa for P_f = 0.95. *Fig. 4* presents the resulting force-displacement curves from the two simulations compared to the eleven experiments. We note that the fracture initiation of all the experiments is within the range predicted by the two simulations. *Fig. 5* presents the resulting crack pattern from the two simulations. Here, we note a clear difference in crack pattern when comparing the P_f = 0.05 simulation to the P_f = 0.95 simulation.

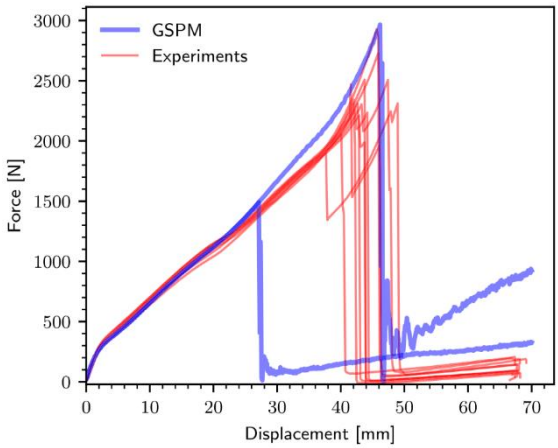

Fig. 4: Force–displacement curves from a possible application of the GSPM expansion of MAT_280 in LS-DYNA compared to experimental data. The P_f = 0.05 and P_f = 0.95 force–displacement curves (in blue) are plotted with the experimental results (in red). Adopted from [6].

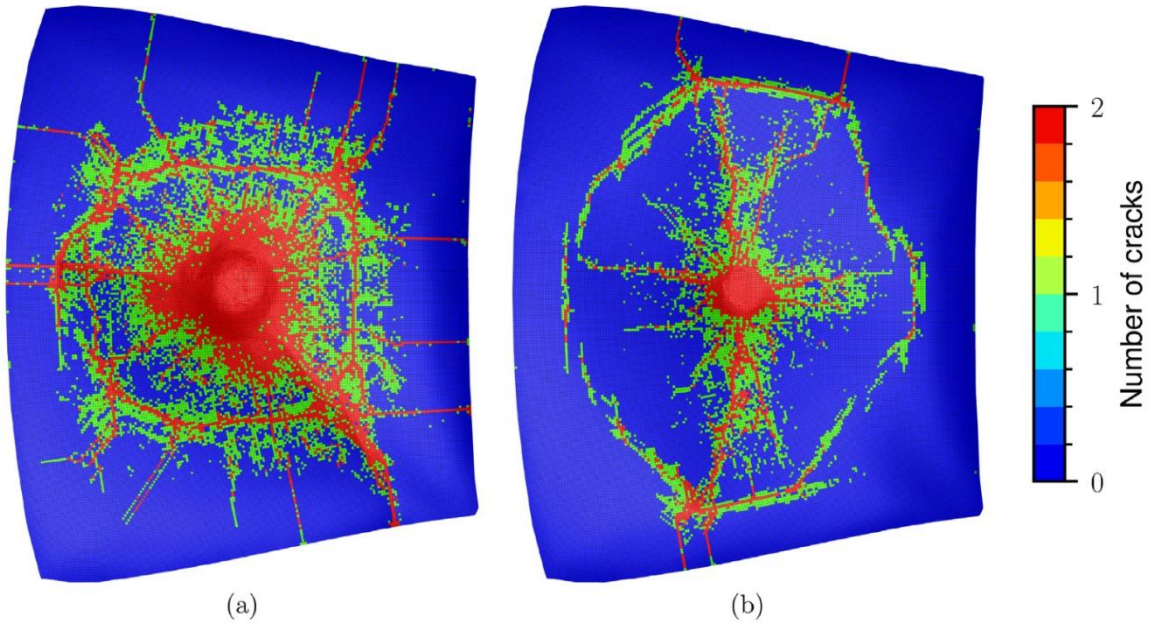

Fig. 5: Resulting crack patterns from the simulations in Fig. 4 displaying a possible application of the GSPM expansion of MAT_280 in LS-DYNA for P_f values of 0.05 (a) and 0.95 (b). Adopted from [6].

4 Summary

The paper provides a brief presentation of the Glass Strength Prediction Model (GSPM), including descriptions of the generation of a representative sample of flaw maps and the overall model procedure. Further, the implementation into LS-DYNA, as an extension of MAT_280 is discussed. To demonstrate the extension, we presented a prediction of the outer limits of the strength of a quasi-statically loaded windshield, were the predictions showed good agreement with the experimental results.

5 References

[1] W. Weibull, «A statistical theory of strength of materials.,» *IVB-Handl,* 1939.

[2] D. Z. Yankelevsky, «Strength Prediction of Annealed Glass Plates – A New Model,» *Eng. Struct.,* vol. 79, pp. 244-255, 2014.

[3] D. Kinsella og E. Serrano, «Failure modelling of glass plates in biaxial loading: using flaw-size based weakest-link systems,» *Glass Struct Eng,* 2021.

[4] NCAP, «Global new car assessment programme (NCAP),» [Internett]. Available: https://www.globalncap.org/. [Funnet 20 3 2023].

[5] C. Brokmann, A Model for the Stochastic Fracture Behavior of Glass and Its Application to the Head Impact on Automotive Windscreens, vol. 63, Springer Fachmedien Wiesbaden, 2022.

[6] J. Rudshaug, K. O. Aasen, O. S. Hopperstad og T. Børvik, «A physically based strength prediction model for glass,» *International Journal of Solids and Structures,* 2023.

[7] K. Osnes, T. Børvik og O. S. Hopperstad, «Shock Tube Testing and Modelling of Annealed Float Glass,» *EPJ Web of Conferences,,* vol. 183, 2018.

[8] K. Osnes, O. S. Hopperstad og T. Børvik, «Rate Dependent Fracture of Monolithic and Laminated Glass: Experiments and Simulations,» *Eng. Struct.,* vol. 212, 2020.

[9] M. Haldimann, Fracture Strength of Structural Glass Elements: Analytical and Numerical Modelling, Testing and Design (Ph.D. thesis), 2006.

[10] A. A. Wereszczak, M. K. Ferber og W. Musselwhite, «Method for Identifying and Mapping Flaw Size Distributions on Glass Surfaces for Predicting Mechanical Response,» *Int. J. Appl. Glass Sci.,* vol. 5, nr. 1, pp. 16-21, 2014.

[11] J. Bentley og B. Floyd, «Programming pearls: a sample of brilliance,» *Communications of the ACM 30.9,* 1987.

[12] J. Rudshaug, O. S. Hopperstad og T. Børvik, «Capturing fracture initiation and crack propagation of car windshields,» *Eng. Fract. Mech.,* 2023.

[13] W. L. Beason, T. L. Kohutek og J. M. Bracci, «Basis for ASTM E 1300 Annealed Glass Thickness Selection Charts,» *J. Struct. Eng.,* vol. 124, nr. 2, pp. 215-221, 1998.

[14] W. L. Beason og J. R. Morgan, «Glass Failure Prediction Model,» *J. Struct. Eng.,* vol. 110, nr. 2, pp. 197-212, 1984.

[15] W. G. Brown, «A Load Duration Theory for Glass Design,» 1972.

[16] W. C. Brown, «A Practicable Formulation for the Strength of Glass and Its Special Application to Large Plates,» pp. 61-p., 1970.

[17] H. C. Chandan, R. C. Bradt og G. E. Rindone, «Dynamic Fatigue of Float Glass,» *J. Am. Ceram. Soc.,* vol. 61, nr. 5-6, pp. 207-210, 1978.

[18] A. G. Evans og S. M. Wiederhorn, «Proof Testing of Ceramic Materials—an Analytical Basis for Failure Prediction,» *Int. J. Fract.,* vol. 10, nr. 3, pp. 379-392, 1974.

[19] A. C. Fischer-Cripps og R. E. Collins, «Architectural Glazings: Design Standards and Failure Models,» *Build. Environ.,* vol. 30, nr. 1, pp. 29-40, 1995.

[20] C. R. Kurkjian, P. K. Gupta og R. K. Brow, «The Strength of Silicate Glasses: What Do We Know, What Do We Need to Know?,» *Int. J. Appl. Glass Sci.,* vol. 1, nr. 1, pp. 27-37, 2010.

[21] W. Lynn Beason og H. Scott Norville, «Development of a New Glass Thickness Selection Procedure,» *J. Wind Eng. Ind. Aerodyn.,* vol. 36, pp. 1135-1144, 1990.

[22] I. Nurhuda, N. Lam, E. F. Gad og I. Calderone, «Estimation of Strengths in Large Annealed Glass Panels,» *Int. J. Solids Struct.,* vol. 47, nr. 18-19, pp. 2591-2599, 2010.

[23] M. Overend og K. Zammit, «A Computer Algorithm for Determining the Tensile Strength of Float Glass,» *Eng. Struct.,* vol. 45, pp. 68-77, 2012.

[24] M. Overend, G. Parke og D. Buhagiar, «Predicting Failure in Glass-a General Crack Growth Model,» *J. Struct. Eng.,* vol. 133, nr. 8, pp. 1146-1155, 2007.

[25] J. E. Ritter Jr. og C. L. Sherburne, «Dynamic and Static Fatigue of Silicate Glasses,» *J. Am. Ceram. Soc.,* vol. 54, nr. 12, pp. 601-605, 1971.

[26] F. A. Veer, P. C. Louter og F. P. Bos, «The Strength of Annealed, Heat-Strengthened and Fully Tempered Float Glass,» *Fatigue Fract. Eng. Mater. Struct.,* vol. 32, nr. 1, pp. 18-25, 2009.

[27] S. M. Wiederhorn, «Influence of Water Vapor on Crack Propagation in Soda-Lime Glass,» *J. Am. Ceram. Soc.,* vol. 50, nr. 8, pp. 407-414, 1967.

[28] W. L. Beason, A Failure Prediction Model for Window Glass (Ph. D. thesis), Texas Tech University, 1980.

[29] M. Pathirana, N. Lam, S. Perera, L. Zhang, D. Ruan og E. Gad, «Risks of failure of annealed glass panels subject to point contact actions,» *International Journal of Solids and Structures,* 2017.

[30] D. Kinsella og K. Persson, «A numerical method for analysis of fracture statistics of glass and simulations of a double ring bending test,» *Glass Struct Eng,* 2018.